An Efficient MLFMA for Accurately Analyzing Electromagnetic Radiation and Coupling Characteristics of Large-scale Antenna Arrays Mounted on Platform

Lei Yin[1], Ning Ding[1], Peng Hou[1], Zhongchao Lin[1], Xunwang Zhao[1], Shugang Jiang[2], and Yongchang Jiao[1]

[1]Shaanxi Key Laboratory of Large Scale Electromagnetic Computing
Xidian University, Xi'an, Shaanxi 710071, China
yinlei@stu.xidian.edu.cn, dn95999@163.com, hou_peng@foxmail.com
zclin@xidian.edu.cn, xwzhao@mail.xidian.edu.cn, ychjiao@xidian.edu.cn

[2]Xi'an CETC-Xidian University Collaborative Innovation Institute of Radar Technology Co. Ltd
Xi'an, Shaanxi 710000, China
zaishuiyifang131@126.com

Abstract **–** A multilevel fast multipole algorithm (MLFMA) for analyzing electromagnetic radiation and coupling characteristics of large-scale antenna arrays mounted on the platforms is presented in this paper. Compared with the method of moments (MoM), the MLFMA can be used to calculate larger scale problems with limited resources. First, waveport model of the MLFMA based on the equivalence principle and mode matching theory is established to efficiently and accurately simulate the antenna array. Then, a preconditioning approach for solving the radiation problems with the waveports is designed to improve convergence of the MLFMA. An initial guess construction method is proposed to accelerate the MLFMA computation for the multi-excitation problems, which can reduce the iteration time by at least 50%. Numerical results demonstrate accuracy and efficiency of the proposed method.

Index Terms **–** electromagnetic radiation and coupling, multilevel fast multipole algorithm (MLFMA), multi-excitation problems, preconditioner, waveport.

I. INTRODUCTION

Electromagnetic (EM) radiation and coupling analysis of large-scale antenna arrays mounted on the platform is an important problem in real-life applications, such as electromagnetic compatibility (EMC) analysis of airborne antennas [1, 2] and optimization of antenna arrays [3, 4]. For the EMC analysis of airborne antennas, the conventional method is to calculate the antenna pattern and S parameters by using the method of moments (MoM) [5], the finite element method (FEM) [6], or the hybrid MoM-physical optics (PO) method [7–9]. In the antenna array optimization problems, the MoM and FEM are used to extract the active element pattern (AEP) for each antenna element [10]. Since the large-scale antenna arrays and platforms lead to a large number of unknowns, the MoM and FEM can hardly be implemented due to the limitation of computational resources, and the hybrid MoM-PO can reduce the consumption of computational resources but cannot satisfy the accuracy requirements for engineering applications. The time-domain EM field calculation methods such as the stabilized DG algorithms are widely used in the simulation of broadband characteristics for ultrawideband (UBW) communication and EMC systems [11–13]. Although these methods can obtain accurate results, they consume huge time resources when calculating electrically large models. Besides, some accurate numerical methods such as the spectral element method (SEM) [14–16] are developed, and SEM is found to be more accurate [17, 18] and could be used for analyzing waveguides and antennas [19, 20]. However, the volume mesh and domain truncation will generate a large number of unknowns, which will lead to excessive consumption of computational resources when calculating the antenna arrays mounted on a large platform. To meet the increasing demands for rapidly designed high-performance antennas and accurate EMC analysis of large-scale arrays, it is imperative to overcome bottlenecks of the existing numerical methods. As a low computational complexity algorithm, the multilevel fast multipole algorithm (MLFMA) can effectively reduce the computation memory and time consumptions [21]. In recent years, thanks to the numerous research works [22–24], capacity and efficiency of the MLFMA have been further significantly improved. However, the

Submitted On: December 16, 2023
Accepted On: April 17, 2024
https://doi.org/10.13052/2024.ACES.J.390309

MLFMA is still weak for solving radiation and coupling characteristics of antenna arrays due to the bottleneck of related techniques. Most of the research on the MLFMA was focused on analyzing the scattering characteristics of metal or dielectric models, and there are still few researches on solving complex antenna radiation problems by using the MLFMA. Furthermore, although some iterative solvers spend lower computational costs in solving the EM problems, the MLFMA still suffers from convergence problems, and an effective and robust preconditioning method for accurately analyzing complex antenna arrays is urgently needed. Moreover, the iterative solvers are inefficient for solving the multi-excitation problems, which require restarting for each right-hand side (RHS).

In this paper, a preconditioned MLFMA oriented to the radiation and coupling analysis for a large-scale antenna array mounted on the platform is presented. First, waveport model of the MLFMA based on the equivalence principle and mode matching theory is established, which can realize the accurate EM modeling for the antenna excitation source and matching load. In this way, the MLFMA can be used for solving the radiation problems with waveports. Then, a preconditioning approach is designed for the MLFMA to analyze the radiation problems with waveport excitations. Moreover, to improve efficiency of the MLFMA when solving multi-excitation problems, an initial guess construction method by extracting typical characteristic currents is proposed. To demonstrate effectiveness and capability of the proposed method, a slot antenna array with a dielectric radome is analyzed, and the proposed initial guess construction method can reduce the iteration time by at least 50%. Finally, a numerical example of an antenna array consisting of 100 dipole antenna elements mounted on a ship is analyzed, validating that the proposed algorithm can simulate large-scale antenna arrays mounted on the platforms under limited computational resources.

II. THEORETICAL ANALYSIS

A. Waveport modeling for MLFMA

To calculate the antenna pattern and S parameters of antenna arrays, the accurate excitation sources model is necessary for the MLFMA. The waveport can be developed to realize the accurate modeling of excitation sources and absorb power of the traveling wave at the matched port. We assume that the semi-infinite waveguides are connected to the original waveguides, and the EM fields propagating to the semi-infinite waveguide will never reflect. In the semi-infinite waveguides, we assumed that the incident wave of a specific mode propagates to the original waveguide, hence the waveports can be used as the excitation sources.

We first establish the integral equations on the boundary surfaces of composite structures, which can be referred to as a multiple region problem. The metal-dielectric models are formulated in terms of the electric field integral equation (EFIE) and the Poggio-Miller-Chang-Harrington-Wu (PMCHW) formulation. As an example, for different regions i and j, the electric fields and magnetic fields can be written as:

$$\hat{n}\times(E_{inc}^{(j)}-E_{inc}^{(i)})=\hat{n}\times\{[\eta_i L^{(i)}(J_i)-K^{(i)}(M_i)] - [\eta_j L^{(j)}(J_j)-K^{(j)}(M_j)]\}, \quad (1)$$

$$\hat{n}\times(H_{inc}^{(j)}-H_{inc}^{(i)})=\hat{n}\times\{[K^{(i)}(J_i)+\frac{L^{(i)}(M_i)}{\eta_i}] - [K^{(j)}(J_j)+\frac{L^{(j)}(M_j)}{\eta_j}]\}, \quad (2)$$

where $\hat{n}$ is the unit normal on the boundary surface from region j to region i, $\eta_i=\sqrt{\varepsilon_i/\mu_i}$ is the wave impedance of region i, and the integral operators L and K are defined as:

$$L(X)=-\int_S(X+\frac{1}{k^2}\nabla\cdot X\nabla)G(r,r')ds', \quad (3)$$

$$K(X)=-\int_S X\times\nabla G(r,r')ds', \quad (4)$$

where k is the wave number, and $G(r,r')$ is the Green function. Equations (1) and (2) are the well-known PMCHW formulation, and Equation (1) can degenerate into the EFIE formulation for modeling metallic waveguides and structures.

Then we formulate the integral equations on the aperture surface S in the original waveguide port. As shown in Fig. 1, the electric field $E^{(p)}$ and magnetic field $H^{(p)}$ satisfy the boundary condition on the surface of S on the origin waveguide side:

$$\hat{n}\times H^{(p)}=J_s, \quad (5)$$

$$\hat{n}\times E^{(p)}=-M_s. \quad (6)$$

Then we formulate the integral equations on the aperture surfaces in the semi-infinite waveguides. Utilizing Schelkunoff's equivalence principle to the semi-infinite waveport region, the currents are related to the tangential fields on outer side of the aperture surface S:

$$-\hat{n}\times H^{(port)}=-J_s, \quad (7)$$

$$-\hat{n}\times E^{(port)}=M_s, \quad (8)$$

since the tangential electric currents impressed on a PEC surface, i.e. J_s, will not radiate. The total fields in the semi-infinite waveguide region consist of three parts, i.e. the incident fields E_{inc} and H_{inc}, the reflected fields produced by the reflection of incident fields, and the fields radiated by M_s. Total fields in the semi-infinite

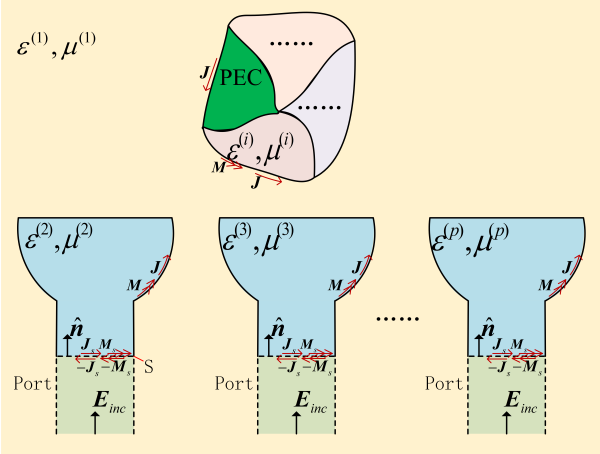

Fig. 1. Composite metallic and dielectric structures with multiport waveguide.

waveguide are expressed as:

$$E^{(port)} = e_j e^{-j\beta_j z} - e_j e^{j\beta_j z} + \sum_{l=1}^{\infty} b_l e_l e^{j\beta_j z}, \quad (9)$$

$$H^{(port)} = \frac{\hat{n}\times e_j}{\eta_j} e^{-j\beta_j z} + \frac{\hat{n}\times e_j}{\eta_j} e^{j\beta_j z} - \sum_{l=1}^{\infty} b_l \frac{\hat{n}\times e_l}{\eta_j} e^{j\beta_j z}, \quad (10)$$

where z is the z-direction distance from the aperture surface, e_j is the normalized eigenvector of the waveguide, and e_l is the lth excitation mode. The fields on the aperture surface with $z = 0$ can be expressed as:

$$E^{(port)}|_{s^-} = \sum_{l=1}^{\infty} b_l e_l, \quad (11)$$

$$H^{(port)}|_{s^-} = \frac{2\hat{n}\times e_j}{\eta_j} - \sum_{l=1}^{\infty} b_l \frac{\hat{n}\times e_l}{\eta_j}. \quad (12)$$

Based on Equations (11), (12) and the boundary condition on the aperture surface in the waveguide $\hat{n}\times H|_{s^+} = (-\hat{n})\times H|_{s^-} = J_s$, the integral equation on the aperture surface can be written as:

$$-\hat{n}\times J_s - \sum_{l=1}^{\infty} \frac{\hat{n}\times e_l}{\eta_j \int_s (\hat{n}\times e_l)\cdot M_s ds} = \frac{2\hat{n}\times e_j}{\eta_j}. \quad (13)$$

The coupled (1) and (2) equations are applied to the original waveguides and the composite structures, Equation (13) is used to model the waveguide ports. The electromagnetic current distributions can be obtained by solving the integral equations using the MLFMA. The scattering parameters can be derived by using the normalized voltage and current:

$$S_{ij} = \sqrt{\frac{\eta_j}{\eta_i}} \int M \cdot (-\hat{n}\times e_i) ds - \delta(i,j). \quad (14)$$

B. Preconditioning approach

When solving complex antenna radiation problems in practical engineering, there often are some complex metal-dielectric structures. For the discretization, we utilize the Rao-Wilton-Glisson basis functions [25] to expand the surface currents, the system matrix of metal-dielectric models under the waveport excitation can be written symbolically as:

$$\left[\begin{array}{ccc:c} Z_{JJ}^{NF} & Z_{JD}^{NF} & Z_{JM}^{NF} & Z_{JP} \\ Z_{DJ}^{NF} & Z_{DD}^{NF} & Z_{DM}^{NF} & Z_{DP} \\ Z_{MJ}^{NF} & Z_{MD}^{NF} & Z_{MM}^{NF} & Z_{MP} \\ \hdashline Z_{PJ} & Z_{PD} & Z_{PM} & Z_{PP} \end{array}\right], \quad (15)$$

where the subscript J corresponds to the equivalent electric currents on the metal surfaces, the subscripts D and M correspond to the equivalent electric and magnetic currents on the dielectric surfaces, and the subscript P corresponds to the equivalent magnetic currents on the waveport surfaces. Since the system matrix (15) usually is not well-conditioned, a preconditioning approach is designed to improve convergence of the large-scale antenna array models under the waveport excitations. During implementation of the MLFMA, the matrix is decomposed into two parts, i.e. Z_{near} and Z_{far}, and the matrix equation is expressed as:

$$(Z_{near} + Z_{far})\cdot I = V, \quad (16)$$

where Z_{near} is the submatrix corresponding to the interaction between the near-field clusters in the lowest level of the MLFMA octree structure, and Z_{far} is the submatrix corresponding to the interaction among the far-field clusters computed approximately with the matrix-vector-product (MVP). The preconditioning matrix is constructed as:

$$A = \left[\begin{array}{cc} Z_{near} & Z_{12} \\ Z_{21} & Z_{PP} \end{array}\right], \quad (17)$$

where $Z_{12} = [Z_{JP}^T, Z_{DP}^T, Z_{MP}^T]^T$ and $Z_{21} = [Z_{PJ}, Z_{PD}, Z_{PP}]$ are two coupling matrices between the waveguide cavity domain and the waveport domain. We compute the preconditioned residual vector $\tilde{r} = A^{-1} r$ in each iteration, and this is accomplished by solving the equation $A\tilde{r} = r$ by using the direct sparse matrix solver MUMPS [26]. It is important to note that the matrix (17) is fixed and does not change when solving the multi-excitation problems, and factorizations of this matrix are only performed once before the iteration starts. Moreover, this method obtains the full inverse matrix of A instead of its approximate inverse matrix, which leads to a better convergence rate than the commonly used ILU and SAI methods [27].

C. Initial guess construction method

As a low computational complexity algorithm, the MLFMA can efficiently reduce the consumption of computational resources when analyzing the electrically large EM models. However, when solving the EM radiation problems with multiple excitations, each excitation corresponds to a V vector, and the iterative solver needs

to restart for each excitation. For the iterative solvers, the vector I in Equation (16) refers to the unknown coefficients of system matrix equation, which is commonly equal to zero before the iteration starts. The conventional method is to use the solution of previous excitation as the initial guess for the next excitation. This method is effectively used in the monostatic radar cross section (RCS) calculations but is ineffective for solving the radiation problems.

In this section, we propose an initial guess construction method for the antenna arrays mounted on a platform to improve convergence of the multi-excitation problems. This method is based on the assumption that electric current distribution of the antenna array is similar when different ports are excited separately. Here, two examples are taken to demonstrate this conclusion intuitively. The first example is an antenna array consisting of 5 slot antennas with the rectangular waveport feeding, as shown in Fig. 2. The second example is a 3×4 dipole antenna array with the coaxial waveport feeding, as depicted in Fig. 4. Both Fig. 3 and Fig. 5 perfectly validate that the electric current distributions have similar characteristics when different ports are excited separately. Based on the above analysis, the initial guess can be constructed by extracting typical characteristic currents from the solution of a given excitation.

For the radiation problems of antenna arrays with N antenna elements mounted on the platform, unknown coefficient vector I of the system matrix equation (16) can be written as:

$$I = [(I^s)^T, (I_k^{sp})^T, (I_k^{wp})^T]^T, k = 1, 2, ..., N, \qquad (18)$$

where I^s denotes unknown coefficient vector of the platform, I_k^{sp} denotes unknown coefficient vector of the k-th antenna waveguide, and I_k^{wp} denotes unknown coefficient vector of the k-th waveport. First, we calculate the solution of one antenna, when that antenna is active and other antennas are passive with an initial value set to zero. To get the most reasonable current distribution possible, usually we first calculate the center element in the array. Then, we extract the typical characteristic currents from the given solution and construct the initial value for the next excitation. The typical characteristic current is

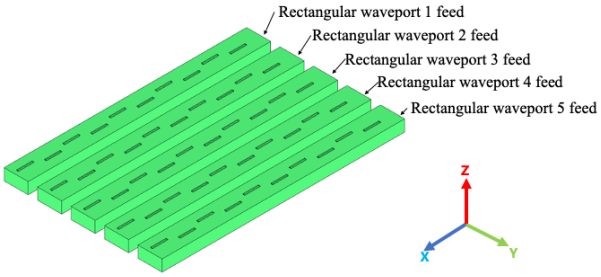

Fig. 2. Slot antenna array simulation model.

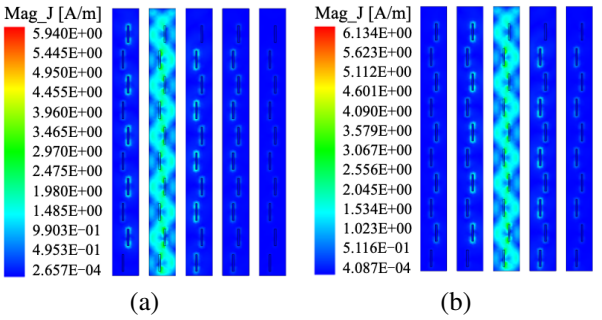

Fig. 3. (a) Electric currents on the surface of slot antenna array with the 2-feed rectangular waveport. (b) Electric currents on the surface of slot antenna array with the 3-feed rectangular waveport.

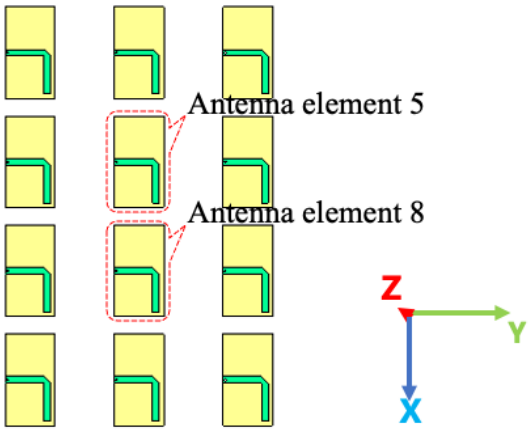

Fig. 4. A 3×4 dipole antenna array model.

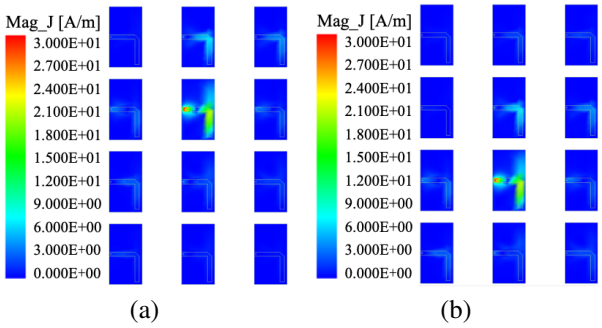

Fig. 5. (a) Electric currents on the surface of dipole antenna array with the 5-feed antenna element. (b) Electric currents on the surface of dipole antenna array with the 8-feed antenna element.

the set of currents of the array center element on the feed port, and the selection criterion can be referred to the S parameter obtained from the first calculation. The typical characteristic current vector I_{typ} extracted from the

solution of the first excitation can be expressed as:

$$I_{typ} = [(I^s)^T, (I_m^{sp})^T, (I_m^{wp})^T]^T, \{m|S_{1,m} > T_s\}, \quad (19)$$

where T_s denotes the threshold for extracting typical characteristic currents, and T_s taken between -20 dB and -30 dB would be appropriate according to the engineering experience. The initial value for the next excitation can be constructed by using I_{typ} and the antenna element in the relative position. For instance, we first obtain the solution when the 3rd antenna is active and other elements are passive, as shown in Fig. 2, and then extract the typical characteristic currents $I_{typ} = [(I^s)^T, (I_{typ}^{sp})^T, (I_{typ}^{wp})^T]^T$ from the solution. We take T_s to be -30 dB in this case, and surface electric currents of the 2nd element, the 3rd element, and the 4th element are chosen to construct I_{typ} according to the S parameters calculated from the first calculation. Hence, the I_{typ}^{sp} and I_{typ}^{wp} can be further expressed as $I_{typ}^{sp} = [0, (I_2^{sp})^T, (I_3^{sp})^T, (I_4^{sp})^T, 0]^T$ and $I_{typ}^{wp} = [0, (I_2^{wp})^T, (I_3^{wp})^T, (I_4^{wp})^T, 0]^T$. We construct the initial value for improving the algorithm convergence when the 2nd element is active, as shown in Fig. 6, by translating I_{typ} according to the antenna element in the relative position, the initial value can be written as $I_{con} = [(I^s)^T, (I_{con}^{sp})^T, (I_{con}^{wp})^T]$, where $I_{con}^{sp} = [(I_2^{sp})^T, (I_3^{sp})^T, (I_4^{sp})^T, 0, 0]^T$ and $I_{con}^{wp} = [(I_2^{wp})^T, (I_3^{wp})^T, (I_4^{wp})^T, 0, 0]^T$. Following this process, we construct a new initial value when the 4th element is active and so on, until we reach the last antenna element.

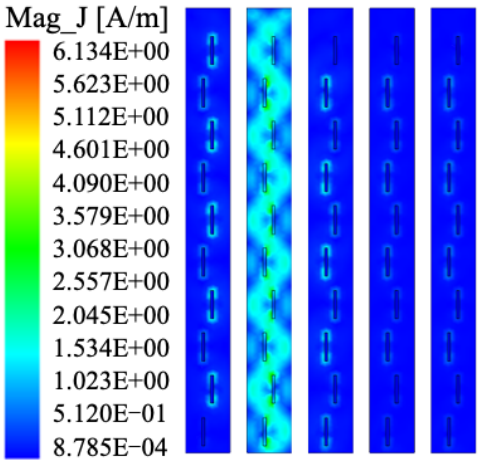

Fig. 6. Initial guess current obtained by reconstructing typical characteristic currents to improve the algorithm convergence when the 2nd antenna element is active.

III. NUMERICAL EXAMPLES

In this section, two examples are performed on a workstation, with 96 CPU cores (Intel Xeon Gold 6248R CPU @ 3.00 GHz) and 1 TB memory. Mean-square-error (MSE) of the directivity is used to compare the numerical accuracy, which is defined as $(\sum_{n=1}^{N} |x_n - x_n^{ref}|^2)/N$, where x_n denotes the nth actual result, and x_n^{ref} denotes the nth reference result.

A. Slot antenna array with dielectric radome

We demonstrate applicability and correctness of the proposed method through the analysis of slot antenna array with the dielectric radome as depicted in Fig. 7. The slot antenna array consists of 5 waveguides shown in Fig. 2. Operating frequency of the antenna is 3 GHz. Figure 8 (a) presents the calculated magnitude of S_{11} parameters for single slot antenna, showing a very good agreement with the commercial software FEKO. The dielectric radome has an inner radius of 540 mm, an outer radius of 600 mm, and a height of 2000 mm. Relative permittivity of the radome material is 1.5 with a loss tangent of 0.001. The number of unknowns is 1 332 741, and the iterative tolerance is set to 1×10^{-3}. The computing resources with 48 CPU cores are used to perform this simulation, and the proposed method requires 586.44 GB memory and 20542.29 s computing time. Results of this simulation have been compared with the commercial software FEKO. Comparisons of the *xoz*-plane and *yoz*-plane radiation patterns obtained by superimposing magnitude and phase of the feed excitation of each antenna element using the superposition principle at 3 GHz are given in Fig. 9. Taking the FEKO solution as a reference,

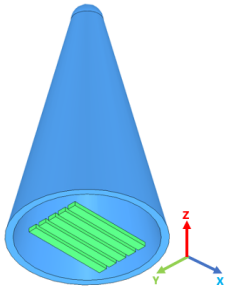

Fig. 7. Simulation model consisting of a waveguide slot antenna array and a dielectric radome.

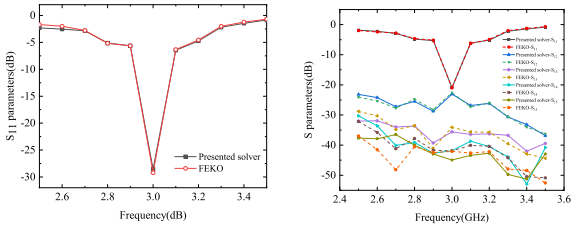

(a) (b)

Fig. 8. (a) Comparison of S_{11} for the single waveguide slot antenna. (b) Comparison of S parameters for the waveguide slot antenna array with dielectric radome.

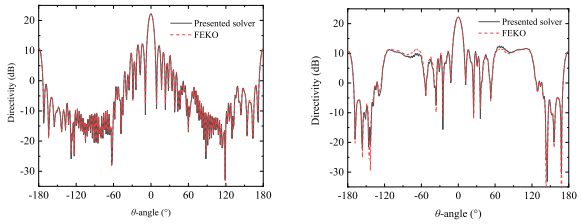

(a) (b)

Fig. 9. Radiation patterns of the waveguide slot antenna array with dielectric radome in the (a) *xoz* plane and (b) *yoz* plane.

MSEs of the directivities in the *xoz*-plane and *yoz*-plane patterns are 0.226 and 0.604, respectively, which show good agreements. Figure 8 (b) shows the calculated magnitude of *S* parameters as a function of frequency, and the iteration steps required by different methods at 3 GHz for this example are given in Table 1. We can see that the conventional method is ineffective for solving the radiation problems, and the proposed method can reduce the computing time for the slot antenna array with radome by at least 50%, showing its effectiveness.

Table 1: Comparison of the iteration steps required by different methods at 3 GHz, when different elements are active. Here, * denotes the antenna element chosen in the first calculation

Active Antenna Element	Initial Value = 0	Conventional Method	Proposed Method
Antenna 1	74	74*	33
Antenna 2	76	74	32
Antenna 3	74	76	74*
Antenna 4	77	76	32
Antenna 5	73	74	31

B. Dipole antenna array mounted on a ship

In the second example, an antenna array mounted on a conducting ship model is analyzed. The antenna array consists of 10×10 dipole antenna elements. This benchmark demonstrates that the proposed method can solve some challenging EM problems as well. The antenna element structure is shown in Fig. 10, and its operating frequency is 3 GHz. Relative permittivity of the dielectric substrate is 4.4 with a loss tangent of 0.02. The conducting ship, as shown in Fig. 11 (a), has a length of 22550 mm, a width of 3024 mm, and a height of 3734 mm. The model is discretized into 3 178 265 unknowns, which require huge hardware resources for

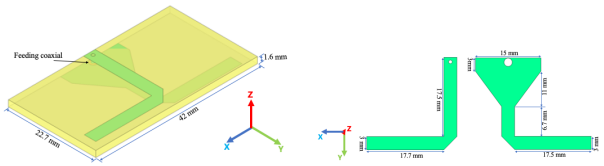

(a) (b)

Fig. 10. Simulation model of the dipole antenna element. (a) Structure of the dipole antenna element. (b) Structure of the PEC patch.

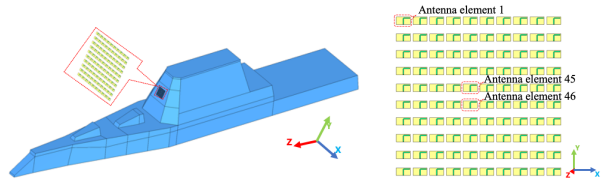

(a) (b)

Fig. 11. Simulation model of the antenna array mounted on a conducting ship. (a) Simulation model of the conducting ship. (b) Simulation model of a 10×10-element antenna array.

the conventional MoM and FEM, and the iterative tolerance is set to 1×10^{-3}. The computing resources with 48 CPU cores are used to perform this simulation. Table 2 presents the hardware resource consumptions and computation times for the array with different cases where all the elements are fed with equal magnitude and same phase. Here, different cases lead to different number of unknowns. In Case 1, the proposed method requires only 319.8 GB memory and 5124.71 s computing time. Figure 12 shows 3-D radiation pattern of the antenna array at 3 GHz obtained by the proposed method, and Fig. 13 shows the near field distribution on the deck of ship. Figure 14 plots the transmission coefficients $S_{45,45}$, $S_{45,46}$, and $S_{45,1}$ in the frequency range of 2.5 GHz to 3.5 GHz (51 sampling points).

Table 2: Comparison of the hardware resource consumptions and computational times for the antenna array mounted on a conducting ship with different cases

	Frequency (GHz)	Number of Unknowns	Memory Usage (GB)	Total Time (s)
Case 1	3	3 178 265	319.8	5124.71
Case 2	4	5 399 778	512.9	6899.89
Case 3	5	8 256 990	558.6	9884.58
Case 4	6	11 749 772	836.2	14180.66

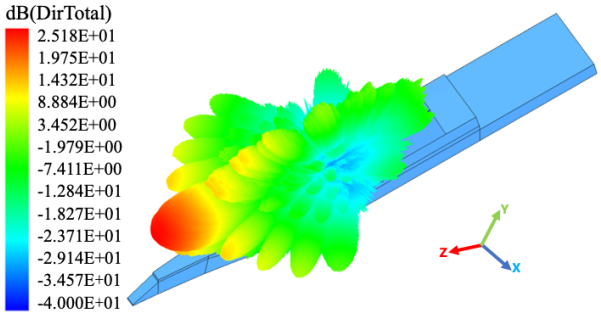

Fig. 12. 3-D radiation pattern of the 10×10-element dipole antenna array mounted on a ship at 3 GHz.

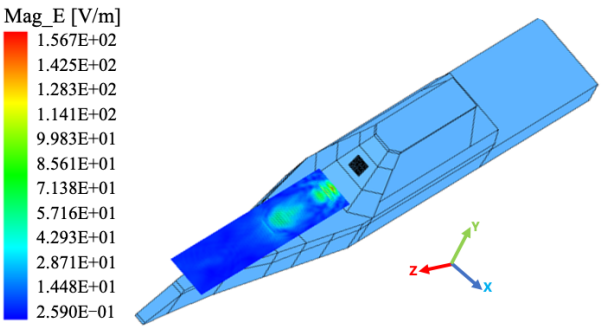

Fig. 13. Near field magnitude distributions on the deck of the ship at 3 GHz.

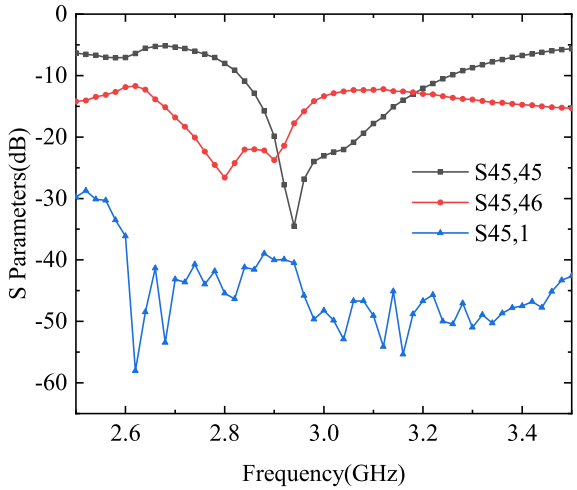

Fig. 14. *S* parameters of the 10×10-element dipole antenna array mounted on a ship.

IV. CONCLUSION

In this paper, an efficient preconditioned MLFMA is presented for analyzing radiation and coupling characteristics of large-scale antenna arrays mounted on electrically large platforms. The waveport model is established for the MLFMA, and a preconditioner is designed for the radiation problems with waveports excitations, which improve the efficiency and convergence for analyzing large-scale antenna arrays. In addition, an initial guess construction method is proposed to effectively analyze coupling problems of the antenna arrays with multiple excitations. Numerical results revealed that the presented method can provide accuracy solutions, and reduce the iteration steps by at least 50% for the multi-excitation problems. Simulation of a 10×10-element antenna array mounted on a conducting ship validates computing power of the method. The proposed method can also be used for calculating the sum and difference beams patterns of antenna arrays with radomes, which also provides an effective method for accurately analyzing radiation and coupling characteristics of the airborne and shipborne antenna arrays.

ACKNOWLEDGMENT

This work is supported in part by the Key Research and Development Program of Shaanxi under Grant 2022ZDLGY02-02, 2021GXLH-02, and 2023-ZDLGY-09, and in part by the Fundamental Research Funds for the Central Universities under Grant QTZX23018.

REFERENCES

[1] C. Zhai, X. Zhao, Z. Lin, and Y. Zhang, "Integrated analysis and optimization of the large airborne Radome-Enclosed antenna system," *Applied Computational Electromagnetics Society Journal*, vol. 35, no. 10, pp. 1192-1199, Oct. 2020.

[2] Z. Lin, Y. Chen, X. Zhao, D. Garcia-Donoro, Y. Zhang, and H. Zhang, "Parallel higher-order method of moments with efficient Out-of-GPU memory schemes for solving electromagnetic problems," *Applied Computational Electromagnetics Society Journal*, vol. 32, no. 9, pp. 781-788, 2017.

[3] P. Zhou, Z. Zhang, and M. He, "Radiation pattern recovery of the Impaired-Radome-Enclosed antenna array," *IEEE Antennas and Wireless Propagation Letters*, vol. 19, no. 9, pp. 1639-1643, 2020.

[4] Y. Liu, M. Li, R. L. Haupt, and Y. J. Guo, "Synthesizing shaped power patterns for linear and planar antenna arrays including mutual coupling by refined joint rotation/phase optimization," *IEEE Transactions on Antennas and Propagation*, vol. 68, no. 6, pp. 4648-4657, 2020.

[5] D. S. Jones, "Field computation by moment methods," *Computer Journal*, vol. 1, no. 1, p. 1, 1969.

[6] J. Jin, "The finite element method in electromagnetics," *Journal of the Japan Society of Applied Electromagnetics*, vol. 1, no. 1, pp. 1-876, 1993.

[7] X. C. Wei and E. P. Li, "Wide-band EMC analysis of on-platform antennas using impedance-matrix interpolation with the moment method-physical optics method," *IEEE Transactions on Electromagnetic Compatibility*, vol. 45, no. 3, pp. 552-556, 2003.

[8] W. Zhao, L. Li, and L. Hu, "Efficient Current-Based hybrid analysis of wire antennas mounted on a large realistic aircraft," *IEEE Transactions on Antennas and Propagation*, vol. 58, no. 8, pp. 2666-2672, 2010.

[9] Z. Liu, X. Wang, and C. Wang, "Installed performance modeling of complex antenna array mounted on extremely large-scale platform using fast MoM-PO hybrid framework," *IEEE Transactions on Antennas and Propagation*, vol. 62, no. 7, pp. 3852-3858, 2014.

[10] L. Dai, Y. J. Xie, C. Zhang, and P. Wu, "Fast optimization of array antenna enclosed by asymmetric radome using AEP combined with enhanced HGAPSO," *Progress In Electromagnetics Research M*, vol. 103, no. 1, pp. 161-171, 2021.

[11] Q. Zhan, Y. Fang, M. Zhuang, M. Yuan, and Q. H. Liu, "Stabilized DG-PSTD method with nonconformal meshes for electromagnetic waves," *IEEE Transactions on Antennas and Propagation*, vol. 68, no. 6, pp. 4714-4726, 2020.

[12] Q. Zhan, Y. Wang, Y. Fang, Q. Ren, S. Yang, W. Yin, and Q. H. Liu, "An adaptive High-Order transient algorithm to solve large-scale anisotropic maxwell's equations," *IEEE Transactions on Antennas and Propagation*, vol. 70, no. 3, pp. 2082-2092, 2022.

[13] M. Li, Q. Wu, Z. Lin, Y. Zhang, and X. Zhao, "Novel parallelization of discontinuous galerkin method for transient electromagnetics simulation based on sunway supercomputers," *Applied Computational Electromagnetics Society Journal*, vol. 37, no. 7, pp. 795-804, 2022.

[14] I. Mahariq, I. H. Giden, S. Alboon, W. H. F. Aly, A. Youssef, and H. Kurt, "Investigation and analysis of acoustojets by spectral element method," *Mathematics*, vol. 10, no. 17, 2022.

[15] I. Mahariq and A. Erciyas, "A spectral element method for the solution of magnetostatic fields," *Turkish Journal of Electrical Engineering and Computer Sciences*, vol. 25, pp. 2922-2932, 2017.

[16] I. Mahariq, "On the application of the spectral element method in electromagnetic problems involving domain decomposition," *Turkish Journal of Electrical Engineering and Computer Sciences*, vol. 25, no. 2, pp. 1059-1069, 2017.

[17] I. Mahariq, H. Kurt, and M. Kuzuoğlu, "Questioning degree of accuracy offered by the spectral element method in computational electromagnetics," *Applied Computational Electromagnetics Society Journal*, vol. 30, no. 07, pp. 698-705, 2021.

[18] I. Mahariq, M. Kuzuoğlu, and I. H. Tarman, "On the attenuation of the perfectly matched layer in electromagnetic scattering problems with the spectral element method," *Applied Computational Electromagnetics Society Journal*, vol. 29, no. 09, pp. 701-710, 2021.

[19] I. Mahariq, I. Arpaci, and M. Kuzuoglu, "Analysis of scattering from perfect electric conducting cylinders by spectral element method," in *2015 Computational Electromagnetics International Workshop (CEM)*, pp. 1-2, Izmir, Turkey, 2015.

[20] I. Mahariq, I. Giden, H. Kurt, O. Minin, and I. Minin, "Strong electromagnetic field localization near the surface of hemicylindrical particles," *Optical and Quantum Electronics*, vol. 50, no. 423, pp. 1-8, 2017.

[21] J. Song, C.-C. Lu, and W. C. Chew, "Multilevel fast multipole algorithm for electromagnetic scattering by large complex objects," *IEEE Transactions on Antennas and Propagation*, vol. 45, no. 10, pp. 1488-1493, 1997.

[22] W. He, Z. Yang, X. Huang, W. Wang, M. Yang, and X. Sheng, "Solving electromagnetic scattering problems with tens of billions of unknowns using GPU accelerated massively parallel MLFMA," *IEEE Transactions on Antennas and Propagation*, vol. 70, no. 7, pp. 5672-5682, 2022.

[23] W.-J. He, Z. Yang, X.-W. Huang, W. Wang, M.-L. Yang, and X.-Q. Sheng, "High-Performance evaluation of the interpolations and anterpolations in the GPU-Accelerated massively parallel MLFMA," *IEEE Transactions on Antennas and Propagation*, vol. 71, no. 7, pp. 6231-6236, 2023.

[24] X. Chen, "An MLFMA-Based eigenmode theory for electromagnetic scattering analysis from electrically large and complex conducting objects," *IEEE Transactions on Antennas and Propagation*, vol. 71, no. 5, pp. 4254-4261, 2023.

[25] S. Rao, D. Wilton, and A. Glisson, "Electromagnetic scattering by surfaces of arbitrary shape," *IEEE Transactions on Antennas and Propagation*, vol. 30, no. 3, pp. 409-418, 1982.

[26] "MUMPS," https://mumps-solver.org, 2023.

[27] L. Gürel, T. Malas, and O. Ergül, "Preconditioning iterative MLFMA solutions of integral equations," in *2010 URSI International Symposium on Electromagnetic Theory*, pp. 810-813, 2010.

Lei Yin was born in Yinchuan, Ningxia, China, in 1995. He received the B.S. degree in electronic and information engineering from Xidian University, Xi'an, China, in 2017. He is currently pursuing the Ph.D. degree with Xidian University, Xi'an, China. His current research interests include computational electromagnetic, parallel computing, and electromagnetic radiation and coupling.

Ning Ding was born in Shanxi, China, in 1995. He received the B.S. degree in electronic and information engineering from Xidian University, Xi'an, China, in 2017. He is currently pursuing the Ph.D. degree with Xidian University, Xi'an, China. His current research interests include computational electromagnetic.

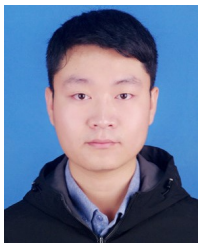

Peng Hou was born in Shaanxi, China, in 1995. He received the B.S. degree in electronic and information engineering from Xidian University, Xi'an, China, in 2017, where he is currently pursuing the Ph.D. degree. His current research interests include computational electromagnetic, parallel computing, and electromagnetic scattering.

Zhongchao Lin was born in Hebei, China, in 1988. He received the B.S. and Ph.D. degrees from Xidian University, Xi'an, China, in 2011 and 2016, respectively. He joined Xidian University, in 2016, as a post doctoral fellow, where he was lately promoted as an associate professor.

His research interests include large-scale computational electromagnetic, scattering, and radiation electromagnetic analysis.

Xunwang Zhao was born in Shanxi, China, in 1983. He received the B.S. and Ph.D. degrees from Xidian University, Xi'an, China, in 2004 and 2008, respectively. He joined Xidian University, in 2008, as a faculty member, where he was lately promoted as a full professor. He was a visiting scholar with Syracuse University, Syracuse, NY, USA, from December 2008 to April 2009. As a principal investigator, he works on several projects, including the project of NSFC. His research interests include computational electromagnetic and electromagnetic scattering analysis.

Shugang Jiang was born in Hebei, China, in 1985. He received the B.S. and Ph.D. degrees from Xidian University, Xi'an, China, in 2008 and 2016, respectively. He joined Xidian University, in 2019, as an associate researcher. His research interests include transient electromagnetic analysis.

Yongchang Jiao was born in Shanxi, China, in 1964. He received the Ph.D. degree in electrical engineering from Xidian University, Xi'an, China, in 1990. Since 1990, he has been with the institute of antennas and EM scattering, Xidian University where he is currently a Professor. From March to June 1996, he was a JSPS visiting priority-area research fellow with the University of Tsukuba, Tsukuba, Japan. From March to September 2002 he was a research fellow with the City University of Hong Kong, Hong Kong. His current research interests include antenna designs, computational electromagnetics, and optimization algorithms.